Predictive Modeling of Risk Associated with Temperature Extremes over North America

UNIVERSITY of WISCONSIN
UWMILWAUKEE
College of Letters and Science
ATMOSPHERIC SCIENCE
DEPARTMENT OF MATHEMATICAL SCIENCES

Sergey Kravtsov, Paul Roebber and Vytaras Brazauskas

Department of Mathematical Sciences, University of Wisconsin-Milwaukee, P.O. Box 413, Milwaukee, WI 53201

AGU FALL MEETING
San Francisco | 12–16 December 2016

Session: NG31A: Stochastic Modeling in Atmosphere, Ocean, and Climate Dynamics
Presentation number: NG31A-1830; Display time: Wednesday, 14 Dec 2016, 08:00-12:20

Introduction

State-of-the-art numerical weather prediction models are expensive to run and are subject to biases due to imperfect physical parameterizations of unresolved processes. An alternative strategy for weather and climate prediction builds on extremely numerically efficient empirical stochastic models, which have recently been shown to be able to capture detailed statistics of select climatic fields of interest (Kravtsov et al. 2016). In this work, we apply this technique to obtain ensemble simulations of surface atmospheric temperature over North America; these simulations will later be used, among other things, to estimate long-term changes in the spatial distribution and magnitude of extreme heat waves and cold spells in the region.

Data sets and methodology

We used surface temperature data set based on National Center for Environmental Prediction North American Regional Reanalysis (http://www.esrl.noaa.gov/psd/gridded/data.narr.html): NARR. The NARR data set is comprised of 3-hourly "observations" on a 349×277 grid with nominal spatial resolution of 32 km, over the 1979–2015 period; about a third of these data are from locations within North America; the resulting data thus has a dimension of ~100000×30000.

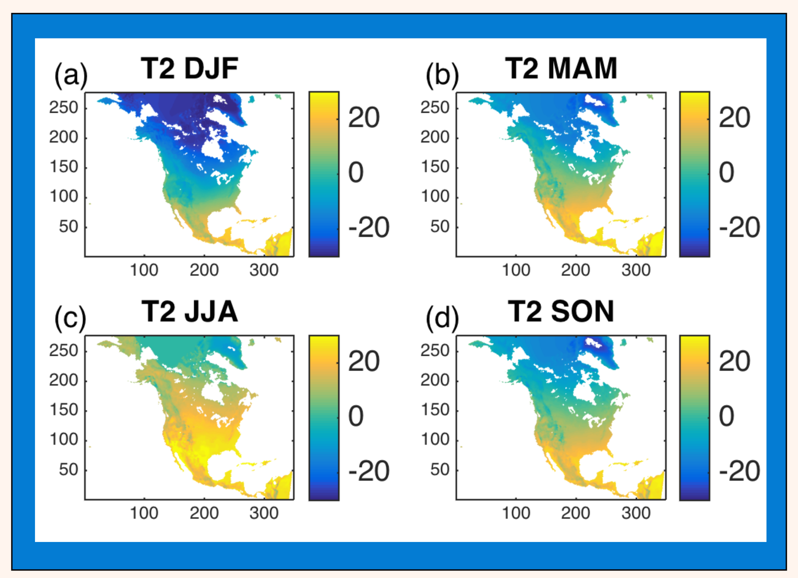

Fig. 1: Seasonal climatology of surface air temperature based on NARR reanalysis.

We subtracted from raw temperature data its seasonal climatology (**Fig. 1**), and built our model in the phase space of surface temperature EOFs (Monahan et al. 2009), to account for over 99% of the total variability. The model's building block is a stochastic ARMA model for the principal components **x**, postulated to have the following multi-level form (Kravtsov et al. 2005) [$d\mathbf{x}=\mathbf{x}^{n+1}-\mathbf{x}^{n}$]:

$$
\begin{aligned}
d\mathbf{x} &= \mathbf{x}\cdot\mathbf{A}^{(1)} + \mathbf{r}^{(1)},\\
d\mathbf{r}^{(1)} &= [\mathbf{r}^{(1)}\,\mathbf{x}]\cdot\mathbf{A}^{(2)} + \mathbf{r}^{(2)}, \qquad (1)\\
d\mathbf{r}^{(2)} &= [\mathbf{r}^{(2)}\,\mathbf{r}^{(1)}\,\mathbf{x}]\cdot\mathbf{A}^{(3)} + \mathbf{r}^{(3)},
\end{aligned}
$$

where the model's parameters are found via regularized multiple linear regression and depend on seasonal cycle at monthly resolution. The model (1) was estimated separately for temperature time series at monthly, daily (for deviations from 3-month means) and three-hourly (for deviations from daily means) resolutions. Input monthly data for the model were obtained by regressing out linear dependence of temperature on external predictors: mean NH temperature, AMO, PDO and Nino3.4 indices. At the stage of simulation, the model was driven by state-dependent noise, whose amplitude was also a function of external predictors. The simulated PCs were transformed back to physical space, with externally forced signal and seasonal climatology added, to provide an emulation of observed variability.

Model performance

We analyze here a single 1979–2015 simulation of the empirical model run from random initial conditions, which produces a synthetic time series of surface temperature on the NARR spatiotemporal grid. This simulation is by construction uncorrelated with the observed data, except for, perhaps, forced signals associated with external predictors.

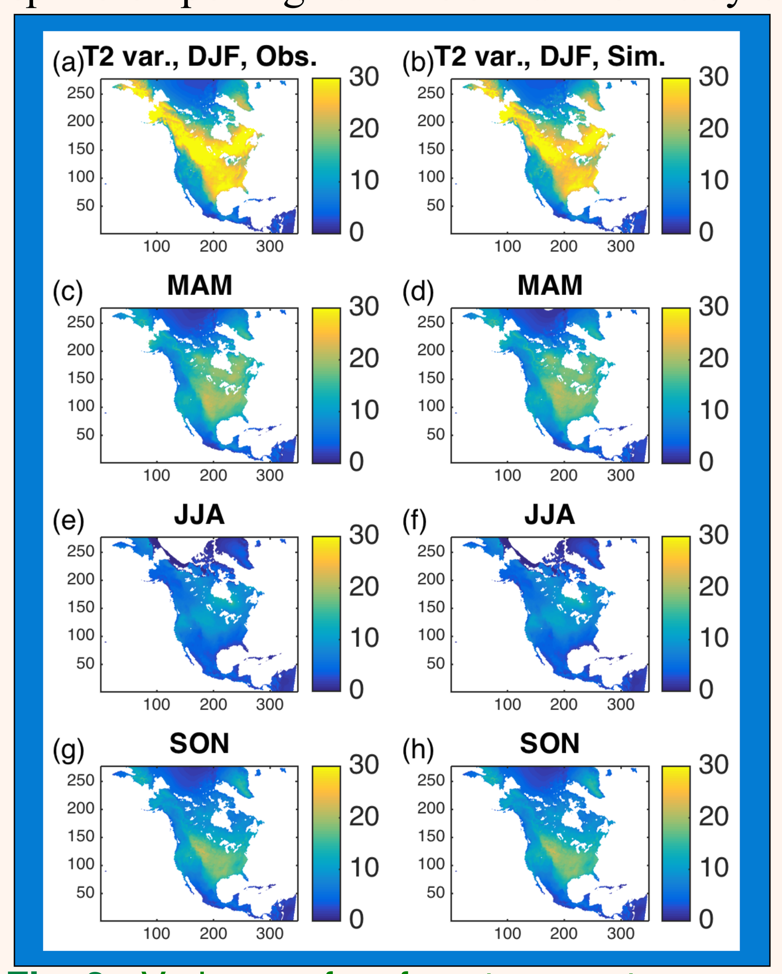

Fig. 2 : Variance of surface-temperature anomalies with respect to climatology (see Fig. 1) in observations (left) and empirical model simulation (right). The model captures well the variance patterns, but underestimates DJF variance.

The model reproduces well the seasonal cycle of temperature variance (**Fig. 2**), albeit it slightly underestimates the magnitude of wintertime variability, primarily due to overly diffusive (in space) cold polar air intrusions from Arctic plains (not shown).

The model also captures quite well the spatial distribution of extreme cold (**Fig. 3**, left) and warm (Fig. 3, right) events. There seems to be, once again, a warm bias in reproducing wintertime extreme cold conditions over the central US (Fig. 3c), possibly related to the variance bias detected in Figs. 2a,b. The bias in hot extremes (Fig. 3f) is less spatially coherent and looks more like sampling variability. We will examine these biases further in ensemble simulations of the empirical model and devise a post-processing procedure to correct for these biases when estimating long-term trends in extreme-event distributions.

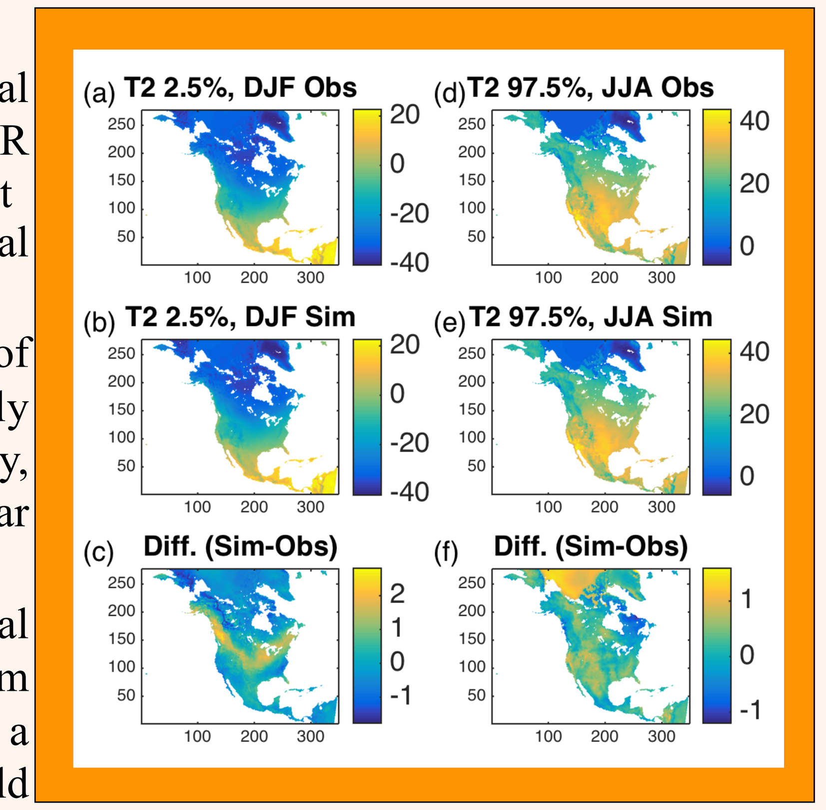

Fig. 3: Extreme events, observed (top) and simulated (middle). The difference between simulations and observations is displayed in the bottom panel. Shown are 37-yr mean of DJF 2.5 (left) and JJA 97.5 percentile of surface temperature for each year.

One of the major advantages of the empirical model considered here is that it is able to capture complex spatiotemporal relationships between the features of the temperature variability associated with forced and internal atmospheric dynamics. **Figure 4** shows examples of anomalous seasonal cold (top three rows) and warm conditions (bottom row). Note that the persistent cold-spell events we have chosen happen in different years in observations and model simulations, which means that they likely stem from the internal dynamics — and are tentatively due to enhanced frequency of synoptic events causing cold-air outbreaks in the months considered. On the other hand, the July 2012 anomalously warm conditions over US Great Plains happen both in observations and in the model simulations, suggesting that this pattern is externally forced (cf. Hoerling et al. 2014; McKinnon et al. 2016). Once again, analysis of ensemble simulations of the empirical model will provide further details on the contributions of forced signals and internal variability to the observed variations of the surface temperature. Finally, **Figure 5** concentrates on daily time scales and shows two analogous examples of the observed and simulated propagating temperature anomalies associated with internal synoptic variability.

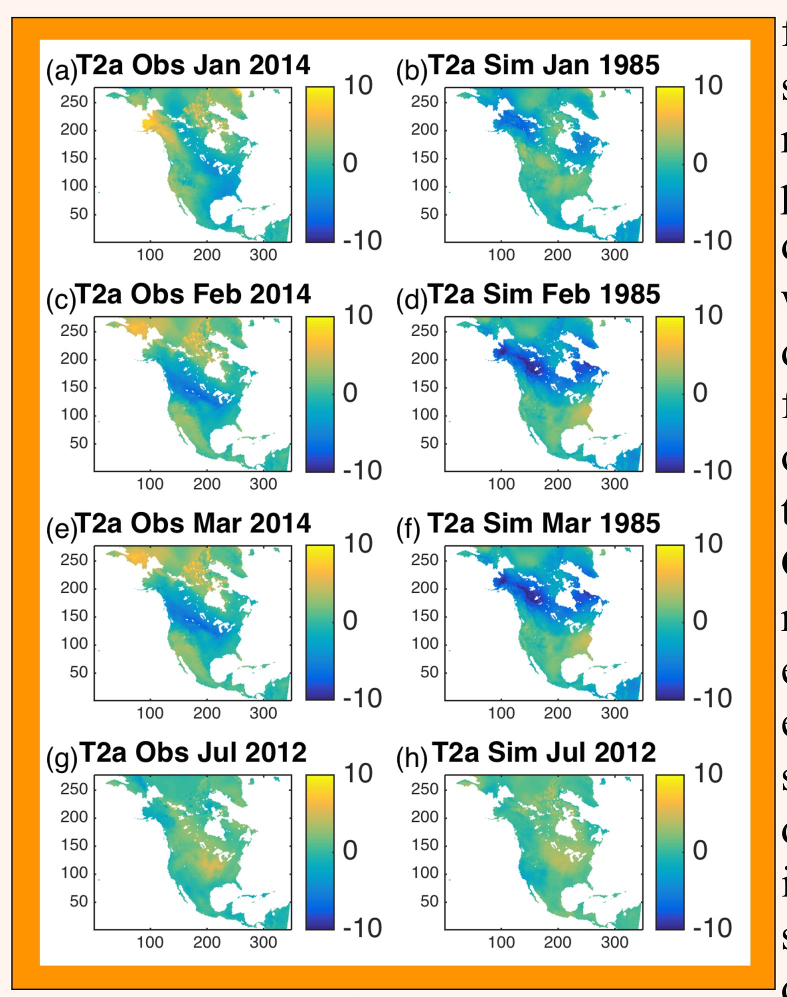

Fig. 4: Examples of monthly surface-temperature anomalies with respect to the seasonal climatology from observations (left) and empirical model simulations (right). The first three rows show a persistent JFM cold spell; the bottom row exemplifies summertime drought conditions.

In summary, our empirical model is able to capture complex spatiotemporal structure and magnitude of the observed temperature variability.

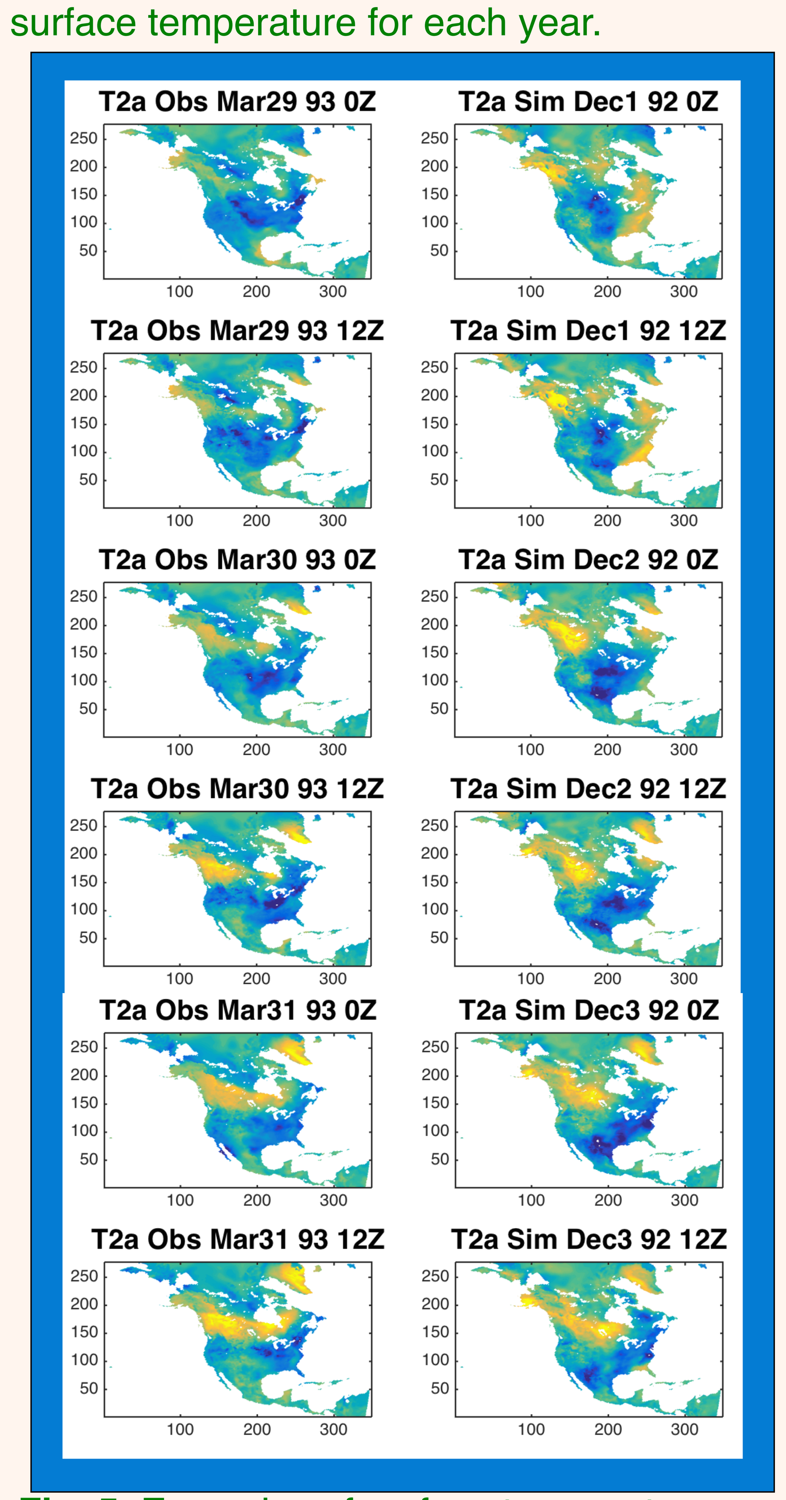

Fig. 5: Examples of surface temperature evolution associated with synoptic events, in observations (left) and simulations (right). The sequence of events in each column spans the period of three days.

Ongoing work

A key advantage of the empirical stochastic model developed here, aside from its excellent performance in reproducing diverse statistical characteristics of the observed surface temperature variability, is its extreme computational efficiency. We have already performed 100 simulations of the entire 1979–2015 period, which took about five days of wall-clock time on a single 2.5GHz processor computer. These simulations will be further utilized to address the following tasks:

- Pinpoint the origin of model biases in simulating the magnitude and distribution of extreme temperature events and develop post-processing bias-correction procedure to alleviate these biases
- Estimate contributions of internal atmospheric dynamics and external forcings in the observed surface-temperature variability
- Obtain (bias corrected) 1979–2015 time series of the cold and warm extreme-event magnitude; examine the trends in the spatial pattern of these events.
- Extrapolate the extreme-event trends into the future decades, both statistically and with the use of sea-surface temperature projections from global models
- Estimate predictability of extreme events

References

Hoerling, M. P., J. Eischeid, A.Kumar, R. Leung, A. Mariotti, K. Mo, S. Schibert and R. Seager, 2014: Causes and predictability of the 2012 Great Plains drought. *Bull. Amer. Meteor. Soc.*, Feb. 2014, 269–282.

Kravtsov, S., D. Kondrashov, and M. Ghil (2005b), Multiple regression modeling of nonlinear processes: Derivation and applications to climatic variability. *J. Climate*, **18**, 4404–4424.

Kravtsov, S., N. Tilinina, Y. Zyulyaeva, and S. Gulev, 2016: Empirical modeling and stochastic emulation of sea-level pressure variability. *J. Appl. Meteor. Climatol.*, **55**, 1197–1219, doi: http://dx.doi.org/10.1175/JAMC-D-15-0186.1.

McKinnon, K. A., A. Rhines, M. P. Tingley and P. Huybers, 2016: Long-lead predictions of eastern United States hot days from Pacific sea-surface temperatures. *Nature Geoscience*, doi: 10.1038/NGEO2687.

Acknowledgments

This research was supported by the Society of Actuaries' Climate Change and Environmental Sustainability Research Committee. SK was also funded by the NSF grants OCE-1243158 and AGS-1408897.

For further information

Please contact *kravtsov@uwm.edu*. A PDF-version of this poster, as well as supplemental figures and animations can be found at http://atmo.math.uwm.edu:8181 → S. Kravtsov Data → KRB2016